Scalable Fabrication of Hierarchically Structured Graphite/Polydimethylsiloxane Composite Films for High-Performance Triboelectric Nanogenerators

Qi-Jun Sun[a], Yanqiang Lei[b], Xin-Hua Zhao[c], Jing Han[b], Ran Cao[b], Wei Wu[a], Hadi Heidari[d], Wen-Jung Li[e], Qijun Sun[b*], and Vellaisamy A. L. Roy[d*]

[a]State Key Laboratory of Terahertz and Millimeter Waves and Department of Materials Science & Engineering, City University of Hong Kong, Kowloon, Hong Kong 999077, China.

[b]Beijing Institute of Nanoenergy and Nanosystems, Chinese Academy of Sciences, Beijing 100083, China.

[c]Department of Chemistry, Southern University of Science and Technology, Shenzhen 518055, China.

[d]James Watt School of Engineering, University of Glasgow, Glasgow, G12 8QQ, United Kingdom.

[e]Department of Mechanical Engineering, City University of Hong Kong, Kowloon, Hong Kong 999077, China.

[*]Corresponding Author:
E-mail: sunqijun@binn.cas.cn (Q. Sun); Roy.Vellaisamy@glasgow.ac.uk (V. A. L. Roy)

Abstract

Health monitoring, e-skin, and soft robotics need energy-harvesting devices to power up their embedded sensors. In this regard, triboelectric nanogenerator (TENG) is an efficient option to energize self-powered sensors and self-charging systems. Herein, a large-scale compatiable and universal bar-assisted printing method is presented to achieve hierarchically microstructured polymer composite triboelectric film with good hydrophobicity to improve the electrical output performance and ambient stability of the TENG. The electrical outputs of the TENG are tuned by imparting the graphite fillers into polydimethylsiloxane (PDMS) and with optimal concentration, the microstructured graphite/PDMS composite based TENG

supplies high and stable short-circuit current of 42 μA, open-circuit voltage of 410 V, and transferred charges of 160 nC under an applied force of 1.2 N, which are sufficient enough to power wearable sensors or charge the energy storage devices. The TENG devices can charge a 2.2 μf capacitor to 1.5 volts within 2 seconds, lighten 30 commercial green LEDs, and drive an electronic watch as well. This work not only demonstrates a scable fabrication of the hierarchically microstructured polymer composite films for high-performance TENGs with high electrical outputs, excellent durability and ambient stability, but also brings insight into the development of future cost-effective and self-powered electronics.

Keywords: energy harvesters, microstructures, polymer composite, scalable fabrication, triboelectric nanogenerators

1. Introduction

Recently, flexible and stretchable sensors have attracted extensive research interest for their promising applications in wearable health monitoring [1-5], skin prosthetics [6-9], and humanoid robotics [10-12]. However, a battery is usually required to power the wearable and portable sensing systems, which is not practical and increases the weight of the whole system. Harvesting energy from ambient environment has been demonstrated as an alternative strategy to solve the above problems [13-20]. Among the energy-harvesting techniques, the triboelectric nanogenerator (TENG) has been proved as a simple and effective paradigm for converting mechanical energy into electricity since it was firstly reported by Wang et al. in 2012 [21]. The working principle of the TENGs can be tracked back to the Maxwell's displacement current [22,23]. TENG is an excellent candidate to supply power for portable and wearable sensing platforms according to its advantages of light weight, excellent flexibility, and structural adaptability [24-30]. To enhance the TENG electric output performance, varieties of strategies are explored such as the optimal device construction, suitable triboelectric materials selection, and microstructure engineering on the friction layer [31-36]. Recently, Tour's group has reported a laser-induced graphene as triboelectric materials for TENG devices with ultra high open-circuit voltage over 3.5 kV and maximum output power of 8 mW [37]. Additionally, Xia et al. have demonstrated that the electric outputs of TENG based on the porous PDMS are significantly improved compared with that of the device based on the pure PDMS film [38]. Despite the notable progress achieved in the development of high-performance TENG, the ambient conditions usually have some negative effects on the triboelectric materials and in turn degrading the TENG electric performance [39,40].

Due to the merits of good chemical stability, excellent flexibility and biocompatibility, polydimethylsiloxane (PDMS) and PDMS-based composites have been widely used for flexible TENGs [41-43]. Additionally, it has been demonstrated that development of

triboelectric films with hierarchical features is one of the efficient solutions to improve the ambient stability and electric outputs of TENGs [44-46]. Recently, tremendous efforts have been devoted to obtaining hierarchically microstructured PDMS or its composite film with a good hydrophobic surface and low surface energy to obstruct the formation of a water skin layer on the surface of the film. Moreover, the microstructures on the PDMS or its composite film can induce obvious change in capacitance change under a compressive force to enhance the electric output performance. However, costly, complicated, and multi-replica processes are mostly required to achieve the hierarchical microstructures possessing good hydrophobic surface, which partially obstructs the TENGs for practical applications. Therefore, it is still highly desired to develop an ambient stable and hierarchically microstructured triboelectric composite film via cost-effective and large-scale compatible approach for high-performance TENGs.

In this work, we present a scalable and universal fabrication strategy to develop the hierarchically microstructured polymer composite with good hydrophobic property to improve the electric outputs and ambient stability of the TENGs. The triboelectric composite film is derived from micron-sized graphite fillers and PDMS matrix, which is achieved by a scalable fabrication process of roller bar-assisted printing. Because of the relatively high viscosity of the PDMS composite inks, we adopted roller bar-assisted printing technique for scalability. For our strategy, the distance between the roller bar and the substrate can be readily controlled to realize a homogeneous thickness of the composite film in a large scale. Compared to the previously reported triboelectric films with microstructures realized via dip-coating, spin-coating or blading approaches, the strategy raised in this work is a universal method to develop the hierarchically microstructured composite films with good homogeneity in a large scale. The hierarchically microstructured composite films developed in this work can be tailored into required size as triboelectric layer in TENGs for various applications. The optimized amount of particle fillers in PDMS matrix can improve the dielectric constant of

the composite film and induce more charges at the surface of friction layers [47]. Therefore, in this work, the electrical performances of the TENGs based on the polymer composites with various filler percentages are investigated to achieve the TENGs with high electrical outputs. Furthermore, the shape and size of the microstructures on the surface of the polymer composite films can influence the electrical performance of TENGs according to the previous reports [48]. Thus, composite films with different surface microstructures were developed to investigate the roughness effects on the TENG electric outputs. In this work, the hierarchically microstructured surface of the polymer composite film is composed of ridges with various hollows which are reversely replicated from the low-cost sandpaper templates. The surface hierarchical ridges can introduce more effective changes in contact area, resulting in more electrostatic charges on the triboelectric layers. Additionally, it is reported that the TENG performance is closely related with the mass ratio of the fillers in the polymer composites [49]. Therefore, the short-circuit current (I_{SC}), open-circuit voltage (V_{OC}), and transferred charges (Q_T) of TENGs are investigated by adjusting graphite mass percentage in the polymer composites. It is demonstrated that the TENG can achieve a high V_{OC} of 410 V, I_{SC} of 42 μA, and Q_T of 160 nC when the mass ratio of graphite to PDMS is 2:5. Moreover, the maximum instantaneous output power of 2.4 mW is achieved at a load resistance of 3 MΩ. The TENG also exhibits good durability with robust electrical outputs even after 15000 loading/unloading cycles and excellent ambient stability over 6 months. To demonstrate their practical applications, the TENGs are used to drive 30 light emitting diodes (LEDs) and wearable electronic watch. This work presents a cost-effective, scalable fabrication of hierarchically microstructured and hydrophobic triboelectric films for high-performance TENGs with fascinating operational and ambient stability. Moreover, the proposed technology may inspire the large-area compatible and cost-effective fabrication of various nano-/micromaterials based polymer composite films for flexible and wearable electronics.

2. Results and Discussion

2.1 Fabrication of the TENG

The fabrication procedures of the TENG device are schematically illustrated in **Figure 1a**. Firstly, the surface of the sandpaper template was cleaned with ethanol and dried with nitrogen gas. Secondly, the polymer composite ink was cast onto one side of a sandpaper template and an indium-tin-oxide (ITO) coated polyethylene terephthalate (PET) film was covered on top. Two plastic spacers with a thickness of 300 μm were inserted between the sandpaper and the ITO/PET film to define the thickness of the polymer composite films. Then, the roller bar of the printer moved horizontally to achieve a uniform polymer composite film between sandpaper and ITO/PET substrate. After that, the printed polymer composite film was annealed in an oven under 90 ^{o}C for 1 h to get the solidified film. Finally, microstructured polymer composite films on ITO/PET substrate were obtained after removing the sandpaper due to the relatively low adhesion between the composite film and the sandpaper. The fabrication processes of the planar G/PDMS composite and the microstructured pure PDMS film were similar with that of G/PDMS composite films. The only differences are changing the sandpaper template with a planar PET substrate for the planar G/PDMS composite and replacing the G/PDMS composite inks with pure PDMS prepolymer, respectively. The pure PDMS or polymer composite film on ITO/PET was cut into regular size (5 cm × 5 cm) as the negative triboelectric layer for the TENG. Another piece of ITO/PET substrate was selected as the positive triboelectric layer with the PET side facing the polymer composite film. Copper wires were attached onto the ITO electrodes from the top and bottom layers to complete the device construction. The scanning electron microscopy (SEM) images shown in **Figure 1b** give the morphologies of graphite fillers, revealing a lateral size ranging from 5 to 20 μm. The morphologies of the sandpaper template and microstructured polymer composite are shown in **Figure 1c** and **d**, respectively. It is observed that the surface of the sandpaper template is composed of hierarchical micro-humps with bigger ones in the size of around 100 μm and

smaller ones in the size of 5-10 μm, respectively. Replicating the reverse structures of sandpaper, hierarchical microstructures were readily achieved for the graphite/PDMS composite. Moreover, the hierarchical microstructured graphite/PDMS composite films were fabricated in a large area of 13 × 13 cm^2 as shown in **Figure S1** (Supporting Information), indicating the scalable fabrication of hierarchical microstructures with a feasible and cost-effective approach.

2.2 Transduction mechanism of the microstructured polymer composite based TENG

The fabricated TENGs in contact-separation mode are composed of a negative layer (G/PDMS or PDMS) and positive layer (PET). During the contact-separation process, the positive layer loses electrons and negative layer tends to get electrons. The working mechanism of our TENG with the microstructured composite film and PET film is schematically depicted in **Figure 2**. In the initial state (**Figure 2-i**), two friction layers are separated and maintain electrically neutral without electrostatically induced charges. When the external compressive force makes the top PET layer contact with the bottom polymer composite layer, same amount of positive and negative charges are induced at the interface of these two layers, respectively. Due to the triboelectric effect, electrons transfer from PET film to G/PDMS film, generating the same amount of positive charges on the PET film. At this stage, no charges flow through the external circuit. When the PET film starts to separate from the G/PDMS film, electrons will flow through the external circuit for charge neutralization. After separation (**Figure 2-ii**), the generated negative charges on top ITO electrode are in the same quantity with the positive charges on bottom ITO electrode due to electrostatic induction. With further separation (**Figure 2-iii**), more negative and positive charges are generated on the top and bottom ITO electrodes to balance the induced charges in triboelectric layers, resulting in a gradually increased output current through the external circuit. Thereafter, as the PET film moves back to the surface of polymer composite film (**Figure 2-iv**), the initial

electrostatic balance is lost, resulting in the electron flow from the top to bottom ITO electrode and a reversed current occurs accordingly. Periodic positive and negative currents are generated in the cyclic compressing and releasing process. The generated electricity by the microstructured polymer composite based TENG can be either directly utilized to drive low-power consuming electronics or restored to drive high power devices assisted with an electrical management circuit.

2.3 Characterization of the TENG devices

To investigate the influence of graphite fillers in the polymer composites on the performance of the TENGs, I_{SC}, V_{OC} and Q_T of the TENGs based on various G/PDMS composite films are studied as shown in **Figure 3a-c**. According to the different concentrations of graphite fillers in the polymer composites, I_{SC}, V_{OC} and Q_T have a similar variation trend. It is observed that the I_{SC}, V_{OC} and Q_T increase with the increased graphite concentration in the composite films and reach the highest values (40 μA, 385 V, 150 nC) when the weight ratio of graphite to PDMS is 2:5, which is almost two times that of the PDMS device (22 μA, 173 V, 65 nC). The improved electric output of the microstructured G/PDMS composite film based devices is ascribed to the improved dielectric constant compared with that of the pristine PDMS film and more induced charges on the surface of the triboelectric layers as shown in **Figure S2** (Supporting Information). However, when the weight percentage of graphite further increases from 2:5 to 5:5, the intensity of the output signals starts to decrease due to partially conductive networks in the composite films [50], which induces leakage currents and decrease the output performance [41,47]. Therefore, in consideration of the TENG output performance, the optimal weight ratio of graphite to PDMS is defined as 2:5.

The I_{SC}, V_{OC} and Q_T of polymer composite film based TENGs are studied in detail. As shown in **Figure 3d-f**, the output performances of the TENGs based on the microstructured and planar G/PDMS composite films are compared. As the hierarchical microstructures on the

G/PDMS composite film can generate more effective contact areas for charge transfer, it enables the microstructured composite based TENG to exhibit an output performance more than twice in comparison with the planar composite film (**Figure 3d-f**). It is noticed that the TENG output performances are dependent on the surface microstructures of the bottom G/PDMS composite layer. Additionally, the influence of composite surface area on the V_{OC} was evaluated by simulating the electric potential distribution using a finite-element method with the COMSOL multiphysics software. The calculated electric potential distributions on the hierarchical G/PDMS composite layer developed from sandpaper templates with different grit sizes are shown in **Figure 3g**. The #200 sandpaper developed composite film based TENG is observed with the largest electric potential difference between the two electrodes under open-circuit conditions. The simulation results agree well with the corresponding experimental results as shown in **Figure S3** (Supporting Information). The effective contact area between the triboelectric films can influence the V_{OC} of the TENGs [48]. In principle, the #80 sandpaper developed composite films have the largest surface area compared with the other composite films. However, the TENG based on the #80 developed G/PDMS composite film shows a low V_{OC}. It should be noted that the V_{OC} depends on the effective contact area change between the triboelectric films rather than the surface area of the triboelectric layer. The compressive force makes the composite film partially contact with the PET film, which likely induces more effective contacts between the #200 sandpaper based G/PDMS composite film and the PET film because of the relatively small roughness of the #200 sandpaper based composite film in comparison with others. Additionally, a reduced V_{OC} of the TENGs based on planar and #400 sandpaper developed G/PDMS composite films is observed, which should be attributed to the reduced surface area of the planar and #400 G/PDMS composite film and in turn a reduced effective contact area under the compressive force. Therefore, under a constant compressive force, the effective contact area change may be comprehensively influenced by the surface area, roughness and mechanical property of the composite films.

Based on the above results, we choose the #200 sandpaper developed G/PDMS composite film as triboelectric film for TENGs. The frequency dependent output signals are also investigated. Based on our previous research, the I_{SC} of a TENG is strongly related with the contact-separation velocity. However, the V_{OC} and Q_T are mainly determined by the displacement [51]. **Figure 4a** shows that the I_{SC} increases with the increased contact-separation frequency and reaches a maximum value of 45 μA at a frequency of 4 Hz. **Figure 4b** illustrates the marginally increased V_{OC} from 340 to 370 V with the frequency increased from 0.5 to 4 Hz. The relatively lower V_{OC} at 0.5 Hz may be attributed to the insufficient surface contact at the low contact-separation frequency. The Q_T also exhibits a similar marginal increase from 131 to 152 nC (**Figure 4c**). Considering the influence of the applied forces, the I_{SC}, V_{OC}, and Q_T of the TENG increase as the force increases from 0.4 to 1.2 N at a frequency of 2 Hz (**Figure 4d-f**). The evaluated average electric outputs per unit area are 1.8 $\mu A \cdot cm^{-2}$ for I_{SC}, 16.8 $V \cdot cm^{-2}$ for V_{OC}, and 7.2 $nC \cdot cm^{-2}$ for Q_T. Recently, Zhang et al. have reported a non-grounded method to measure the V_{OC} of the TENGs [52]. A larger actual V_{OC} of the TENG is expected by using their method as shown in **Figure S4** (Supporting Information). The achieved TENG output performances are sufficient to directly drive low-power electronics and drive high-power devices assisted with a power management circuit. Additionally, the electrical output of the TENG device based on the large size composite (13 × 13 cm^2) has been investigated as shown in **Figure S5**. It is observed that the Voc, I_{SC} and Q_T of the enlarged device are obviously improved compared with those of the device based on 5 × 5 cm^2 composite. Therefore, the TENG device with enlarged size is more efficient in energy harvesting. In contrast, scaling down the TENG size is more benificial for high resolution senisng appications [53].

To assess the output power of G/PDMS composite based TENG, the V_{OC} and I_{SC} with various external loads are measured as shown in **Figure 4g**. The effective output power of the TENG can be calculated by the following equation: $P=U^2/R$, where U and R are the output

voltage and load resistance, respectively. It is observed that the output voltage increases with increasing the external load while a decrease in current is observed according to Ohm's law. As shown in **Figure 4h**, a maximum output power of 2.4 mW under a loading resistance of 3 MΩ is achieved. To drive the portable electronics, the mechanical energy harvested from the ambient environments is generally stored in capacitors in advance. In this work, the charging capacity of the G/PDMS composite based TENG is also evaluated by charging different capacitors (2.2, 10, 47, and 110 μF). As shown in **Figure 4i**, it requires only 2 s to charge a 2.2 μF capacitor up to a voltage of 1.5 V and requires 95 s to charge the 110 μF capacitor up to 1.5 V.

2.4 Applications of the microstructured polymer composite based TENG

To demonstrate practical powering applications of the G/PDMS composite based TENGs, they are used to drive LEDs and an electronic watch. In order to power portable electronic devices continuously, electric management circuits (EMC) have been reported to convert the intrinsic alternating output signals of the TENG to stable and direct outputs. Other types of power managemen circuits (PMC) based on passive electronic components including an inductor, a diode and a capacitor [54] and PMC consisting of a rectifier bridge, an inductor (L), and a capacitor [55] are also excellecnt candidates for more efficient power conversion. As shown in the equivalent electronic circuit (**Figure 5a**), the alternating current (AC) generated by TENGs is converted to direct current (DC) output by a full bridge rectifier to drive the LEDs. It is observed that the TENG can illuminate 30 commercial LEDs connected in series under a contact-separation frequency of 3 Hz (**Figure 5b** and **Movie S1**, Supporting Information). In order to drive the electronic watch continuously, the alternating output signals should be converted to the stable and direct output signals by an electric management circuit (EMC) as depicted in **Figure 5c**. The TENG first charges a 10 μF capacitor and then drives an electronic watch as shown in **Figure 5d** and **Movie S2** (Supporting Information). The voltage of the capacitor can reach 5.5 V within 40 s when the TENG is tapped at a

frequency of 3 Hz. Consequently, the power provided by the TENG is able to drive the watch continuously. All these results indicate that the developed hierarchically structured G/PDMS composite films are effective to be utilized as TENG friction layer to harvest mechanical energy and functionalize in a self-powered system to drive the portable electronics sustainably.

2.5 Durability and ambient stability of the TENG

Furthermore, the durability of the TENG is also investigated. The V_{OC} durability of the TENG is evaluated by a repetitive contact-separation test up to 15,000 cycles at a frequency of 3 Hz, exhibiting a stable voltage output (**Figure 5e**). The insets in **Figure 5e** show the enlarged view of the V_{OC} at the initial and final stage of the test. It is noticed that a high signal-to-noise voltage is maintained and no obvious signal decay is observed, revealing the stable output of our TENGs. For the ambient stability investigation, the TENGs are stored in the ambient condition (Humidity~30%, T~25 ^{o}C) up to 6 months and the output signals are collected once per month as shown in **Figure 5f-i**. No obvious degradations of V_{OC}, I_{SC} and Q_T are observed when the TENGs are stored in the ambient condition up to 6 months, which is attributed to the chemical stability and hydrophobic properties of the microstructured G/PDMS composite film. The water contact angle of the planar and hierarchically microstructured G/PDMS composite films was characterized as shown in **Figure S6** (Supporting Information). An enhanced water contact angle for hierarchically microstructured G/PDMS composite film is observed compared with the that of the planar film, which consists with the previous reports [48]. Furthermore, the humidity resistance of the TENGs based on the planar and hierarchically microstructured G/PDMS composite films were characterized under humidity of 80% as shown in **Figure S7** (Supporting Information). Under 80% humidity, the V_{OC} decreases by 25% and 16% for the TENGs based on the planar and hierarchically microstructured G/PDMS composite films, respectively. This improved humidity stability of the TENG based on the hierarchically microstructured should be attributed to the excellent hydrophobic surface which obstructs the formation of a water skin

layer on the surface of the composite film. The resistance to corrosion ability of the TENG is highly desired for specific applications. In order to demonstrate the stability of our TENGs in liquid medium, the composite film layer was soaked in the DI-water, acid solution, and aqueous alkali for 15 min, respectively. The composite layer was then dried with nitrogen and vacuum oven before assembled into TENG for further measurement. As shown in **Figures 6a**,**b**, the TENG dipped in DI-water shows negligible degradation in V_{OC} compared with the pristine device, which is attributed to the hydrophobic property of the polymer composite film (**Figure S6**, Supporting Information). It is observed with less than 10% degradation in V_{OC} for the TENGs based on the acid or alkali solution soaked composite layer. Additionally, the I_{SC} of the TENGs when exposed to different aqueous solutions is shown in **Figure S8** (Supporting Information), exhibiting the same trend with that of V_{OC}. The above results prove that the TENGs based on the microstructured G/PDMS composite layers exhibit excellent stability against several aqueous solutions, indicating the great potential of our TENGs for the wearable and washable electronic systems.

3. Conclusion

In summary, we present a scalable fabrication of the hierarchically microstructured G/PDMS composite films with good hydrophobicity for high performance TENGs in harvesting mechanical energy. By adjusting the graphite concentration, the TENGs with the optimized polymer composite film achieve relatively high electric output (Voc = 410 V, Isc = 42 μA, and Q_T = 160 nC) and a maximum power of 2.4 mW with an external load of 3 MΩ. Additionally, the TENGs are successfully employed to drive commercial LEDs and an electronic watch to show the practical applications. Furthermore, the TENGs have been demonstrated with excellent stability in ambient conditions and a strong tolerance for various liquids. The technique presented in this work could contribute significantly to advance the

development of high performance and cost-effective energy harvesters with great potential in self-powered wearable sensors and self-charging systems.

4. Experimental Section

4.1 Materials

The polydimethylsiloxane (PDMS, Sylgard 184) was purchased from Dow Corning Co., Ltd. Graphite powder was provided by Beijing Jinglong Tetan Technology Co., Ltd. The indium-tin-oxide coated polyethylene terephthalate (ITO/PET) films with a thickness of 100 μm were provided by South China Science and Technology Co., Ltd. The sandpapers with different grit numbers were obtained from Hong Kong Ruixin Technology Co., Ltd.

4.2 Preparation of polymer composite inks

Firstly, the liquid PDMS base and the curing agent were mixed at a weight ratio of 10:1 to obtain the prepolymer. Secondly, to obtain the composite inks with different compositions, various weights (1, 2, 3, 4 and 5 g) of graphite powder fillers were added in 5 g PDMS prepolymer and thoroughly mixed, respectively. Thirdly, the polymer composite ink was put in a gentle vacuum condition to remove the generated air bubbles inside the ink.

4.3 Characterization of graphite, G/PDMS polymer composite film, and TENGs

Morphologies of graphite fillers and G/PDMS polymer composite films were characterized by FESEM (JSM-6490). The output performance of TENGs was characterized by a measurement system containing a motorized test stand (Winnemotor, WMUC512075-06-X) to control the contact separation frequency, and electrical signals were collected by a semiconductor parameter analyzer (Keithley 6514, Tektronix Inc., USA). The capacitance of the composite films were characterized with HP 4284A LCR meter to calculate the relative dielectric constant. The hydrophobicity of the surface of the composite film was measured by a contact angle goniometer. The ambient stability of the TENG were investigated by dipping the polymer composite films into DI-water, acid solution, and aqueous alkali for 15 min,

respectively. After that, the composite films were dried with nitrogen and annealled in a vacuum oven at 60 ^{o}C for 1 h. Finally, the composite films were assembled into TENGs for further characterization.

Acknowledgements

Q. J. Sun and Y. Q. Lei contributed equally to this work. The authors acknowledge the grant from the Research Grant Council of HKSAR (Grant No. CityU 11210819). Prof. Q. Sun acknowledges the grant from National Key Research and Development Program of China (2016YFA0202703) and Beijing Nova Program (Z191100001119047). We would like thank Siew-Mei Chin and Ka-Wai Kong from City University of Hong Kong for the contact angle measurement.

Appendix A. Supporting Information

Supporting materials are available in the online version of this paper.

References

[1] Y. J. Hong, H. Jeong, K. W. Cho, N. Lu, D. H. Kim, Adv. Funct. Mater. 29 (2019) 1808247.

[2] C. Wang, K. Xia, H. Wang, X. Liang, Z. Yin, Y. Zhang, Adv. Mater. 31 (2019) 1801072.

[3] M. A. O'Mara, S. P. Ogilvie, M. J. Large, A. A. Graf, A. C. Sehnal, P. J. Lynch, J. P. Salvage, I. Jurewicz, A. A. K. King, A. B. Dalton, Adv. Funct. Mater. (2020) 2002433.

[4] Z. Lou, S. Chen, L. Wang, K. Jiang, G. Shen, Nano Energy 23 (2016) 7.

[5] Y. Wang, M. Chao, P. Wan, L. Zhang, Nano Energy 70 (2020) 104560.

[6] D. J. Lipomi, M. Vosgueritchian, B. C-K. Tee, S. L. Hellstrom, J. A. Lee, C. H. Fox, Z. Bao, Nat. Nanotech. 6 (2011) 788.

[7] S. Lee, A. Reuveny, J. Reeder, S. Lee, H. Jin, Q. Liu, T. Yokota, T. Isoyama, Y. Abe, Z. Suo, T. Someya, Nat. Nanotech. 11 (2016) 472.

[8] G. Y. Bae, S. W. Pak, D. Kim, G. Lee, D. H. Kim, Y. Chung, K. Cho, Adv. Mater. 28 (2016) 5300.

[9] L. Wang, J. A. Jackman, E. L. Tan, J. H. Park, M. G. Potroz, E. Hwang, N. J. Cho, Nano Energy 36 (2017) 38.

[10] Y. Cheng, Y. Ma, L. Li, M. Zhu, Y. Yue, W. Liu, L. Wang, S. Jia, C. Li, T. Qi, J. Wang, Y. Gao, ACS Nano 14 (2020) 2145.

[11] Y. Ling, T. An, L. W. Yap, B. Zhu, S. Gong, W. Cheng, Adv. Mater. 32 (2020) 1904664.

[12] Y. Pang, K. Zhang, Z. Yang, S. Jiang, Z. Ju, Y. Li, X. Wang, D. Wang, M. Jian, Y. Zhang, R. Liang, H. Tian, Y. Yang, T.-L. Ren, ACS Nano 12 (2018) 2346.

[13] X. Lu, Y. Xu, G. Qiao, Q. Gao, X. Zhang, T. Cheng, Z. L. Wang, Nano Energy 72 (2020) 104726.

[14] L. Jin, X. Xiao, W. Deng, A. Nashalian, D. He, V. Raveendran, C. Yan, H. Su, X. Chu, T. Yang, W. Li, W. Yang, J. Chen, Nano Lett. (2020) https://dx.doi.org/10.1021/acs.nanolett.0c01987.

[15] H. Kang, C. Zhao, J. Huang, D. H. Ho, Y. T. Megra, J. W. Suk, J. Sun, Z. L. Wang, Q. Sun, J. H. Cho, Adv. Funct. Mater. 29 (2019) 1903580.

[16] G. Khandelwal, N. P. Maria Joseph Raj, S.-J. Kim, Nano Today 33 (2020) 100882.

[17] J. Kim, H. Ryu, J. H. Lee, U. Khan, S. S. Kwak, H. J. Yoon, S. W. Kim, Adv. Energy Mater. 10 (2020) 1903524.

[18] W. Wang, A. Yu, X. Liu, Y. Liu, Y. Zhang, Y. Zhu, Y. Lei, M. Jia, J. Zhai, Z. L. Wang, Nano Energy 71 (2020) 104605.

[19] X. Xiao, L. Yuan, J. Zhong, T. Ding, Y. Liu, Z. Cai, Y. Rong, H. Han, J. Zhou, Z. L. Wang, Adv. Mater. 23 (2011) 5440.

[20] G. Yao, L. Xu, X. Cheng, Y. Li, X. Huang, W. Guo, S. Liu, Z. L. Wang, H. Wu, Adv. Funct. Mater. 30 (2019) 1907312.

[21] F. R. Fan, Z. Q.Tian, Z. L. Wang, Nano Energy 1 (2012) 328.

[22] Z. L. Wang, Nano Energy 68 (2020) 104272.

[23] Z. L. Wang, Mater. Today 20 (2017) 74.

[24] A. Chen, C. Zhang, G. Zhu, Z. L. Wang, Adv. Sci. (2020) 2000186.

[25] X. Ji, P. Fang, B. Xu, K. Xie, H. Yue, X. Luo, Z. Wang, X. Zhao, P. Shi, Nano Lett. 20 (2020) 4043.

[26] H. Guo, X. Pu, J. Chen, Y. Meng, M. Yeh, G. Liu, Q. Tang, B. Chen, D. Liu, S. Qi, C. Wu, C. Hu, J. Wang, Z. L. Wang, Sci. Robot. 3 (2018) eaat2516.

[27] H. Guo, M. Yeh, Y. Zi, Z. Wen, J. Chen, G. Liu, C. Hu, Z. L. Wang, ACS Nano 11, (2017) 4475.

[28] X. Chen, X. Xie, Y. Liu, C. Zhao, M. Wen, Z. Wen, Adv. Funct. Mater. (2020) 2004673.

[29] H. Guo, M. Yeh, Y. Lai, Y. Zi, C. Wu, Z. Wen, C. Hu, Z. L. Wang, ACS Nano 10 (2016) 10580.

[30] K. Zhao, B. Ouyang, C. R. Bowen, Z. L. Wang, Y. Yang, Nano Energy 71 (2020) 104632.

[31] K. Y. Lee, J. Chun, J.-H. Lee, K. N. Kim, N.-R. Kang, J.-Y. Kim, M. H. Kim, K.-S. Shin, M. K. Gupta, J. M. Baik, S.-W. Kim, Adv. Mater. 26 (2014) 5037.

[32] X. W. Zhang, G. Z. Li, G. G. Wang, J. L. Tian, Y. L. Liu, D. M. Ye, Z. Liu, H. Y. Zhang, J. C. Han, ACS Sustainable Chem. Eng. 6 (2018) 2283.

[33] J. Du, X. Yang, J. Duan, Y. Wang, Q. Tang, Nano Energy 70 (2020) 104514.

[34] Y. Wang, S. Gao, W. Xu, Z. Wang, Adv. Funct. Mater. (2020) 1908252.

[35] J. Kim, H. Ryu, J. Lee, U. Khan, S. Kwak, H. Yoon, S. Kim, Adv. Energy Mater. (2020) 1903524.

[36] W. Wang, A. Yu, X. Liu, Y. Liu, Y. Zhang, Y. Zhu, Y. Lei, M. Jia, J. Zhai, Z. L. Wang, Nano Energy 71 (2020) 104605.

[37] M. G. Stanford, J. T. Li, Y. Chyan, Z. Wang, W. Wang, J. M. Tour, ACS Nano 13 (2019) 7166.

[38] X. Xia, J. Chen, H. Guo, G. Liu, D. Wei, Y. Xi, X. Wang, C. Hu, Nano Res.10 (2017) 320.

[39] D. Kim, S. Lee, Y. Ko, C. H. Kwon, J. Cho, Nano Energy 44 (2018) 228.

[40] R. Wen, J. Guo, A. Yu, J. Zhai, Z. L. Wang, Adv. Funct. Mater. 29 (2019) 1807655.

[41] Y. J. Fan, X. S. Meng, H. Y. Li, S. Y. Kuang, L. Zhang, Y. Wu, Z. L. Wang, G. Zhu, Adv. Mater. 29 (2017) 1603115.

[42] K. Ke, C. Chung, Small (2020) 2001209.

[43] G. Li, G. Wang, D. Ye, X. Zhang, Z. Lin, H. Zhou, F. Li, B. Wang, J. Han, Adv. Electron. Mater. (2019) 1800846.

[44] M. S. U. Rasel, J. Y. Park, Appl. Energy 206 (2017) 150.

[45] Z. H. Lin , G. Cheng, Y. Yang , Y. S. Zhou , S. Lee , Z. L. Wang, Adv. Funct. Mater. 24 (2014) 2810.

[46] S. A. Shankaregowda , R. F. Ahmed, Y. Liu , C. B. Nanjegowda , X. Cheng , S. Shivanna , S. Ramakrishna , Z. Yu , X. Zhang , K. Sannathammegowda, Nanomaterials 9 (2019) 1585.

[47] X. Xia, J. Chen, G. Liu, M. S. Javed, X. Wang, C. Hu, Carbon 111 (2017) 569.

[48] D. Kim, S. Lee, Y. Ko, C. H. Kwon, J. Cho, Nano Energy 44 (2018) 228.

[49] M. K. Kim, M. S. Kim, H. B. Kwon, S. E. Jo, Y. J. Kim, RSC Adv. 7 (2017) 48368.

[50] Q. J. Sun, X. H. Zhao, Y. Zhou, C. C. Yeung, W. Wu, S. Venkatesh, Z. X. Xu, J. J. Wylie, W. J. Li, V. A. L. Roy, Adv. Funct. Mater. 29 (2019) 1808829.

[51] Y. Yang, J. Huang, J. Sun, Z. L. Wang, S. Seo, Q. Sun, Adv. Funct. Mater. (2020) 1909652.

[52] W. Zhang, G. Gu, H. Qin, S. Li, W. Shang, T. Wang, B. Zhang, P. Cui, J. Guo, F. Yang, G. Cheng, Z. Du, Nano Energy 77 (2020) 105108.

[53] Y. Liu, L. Wang, L. Zhao, K. Yao, Z. Xie, Y. Zi, X. Yu, Adv. Electron. Mater. (2019) 1901174.

[54] H. Qin, G. Cheng, Y. Zi, G. Gu, B. Zhang, W. Shang, F. Yang, J. Yang, Z. Du, Z. L. Wang, Adv. Funct. Mater. 28 (2018) 1805216.

[55] H. Qin, G. Gu, W. Shang, H. Luo, W. Zhang, P. Cui, B. Zhang, J. Guo, G. Cheng, Z. Du, Nano Energy 68 (2020) 104372.

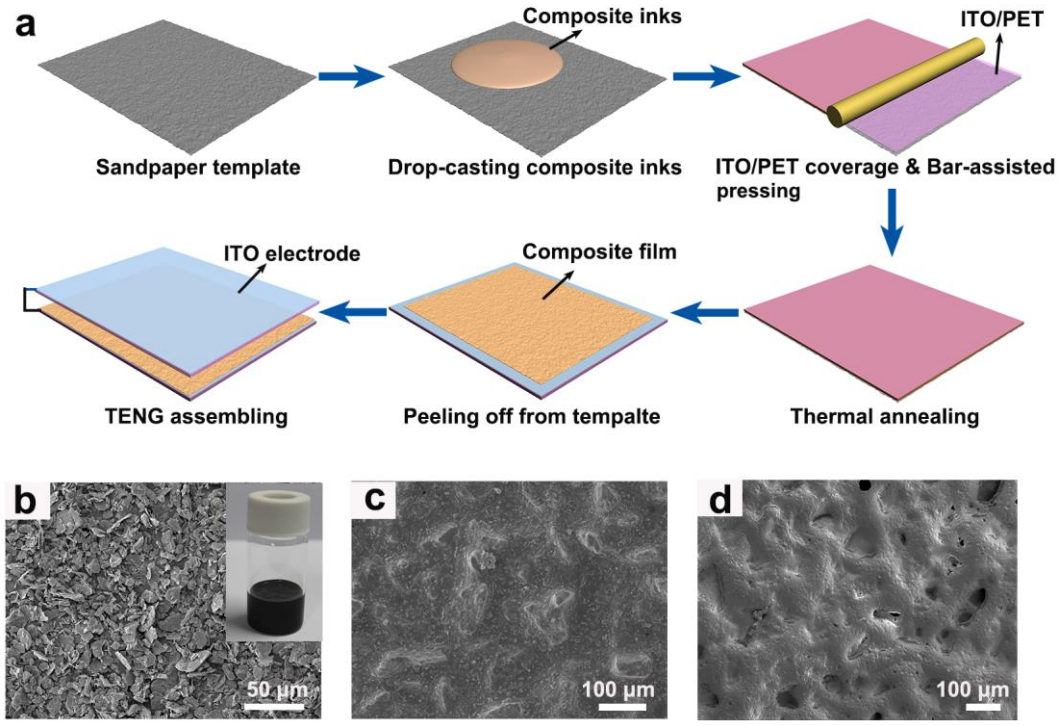

Figure 1. a) Schematic illustration of the whole fabrication process for the microstructured polymer composite based TENG. b) SEM images of graphite powder. Inset showing the composite ink in a bottle. c) and d) SEM images of sandpaper template and microstructured polymer composite film, respectively.

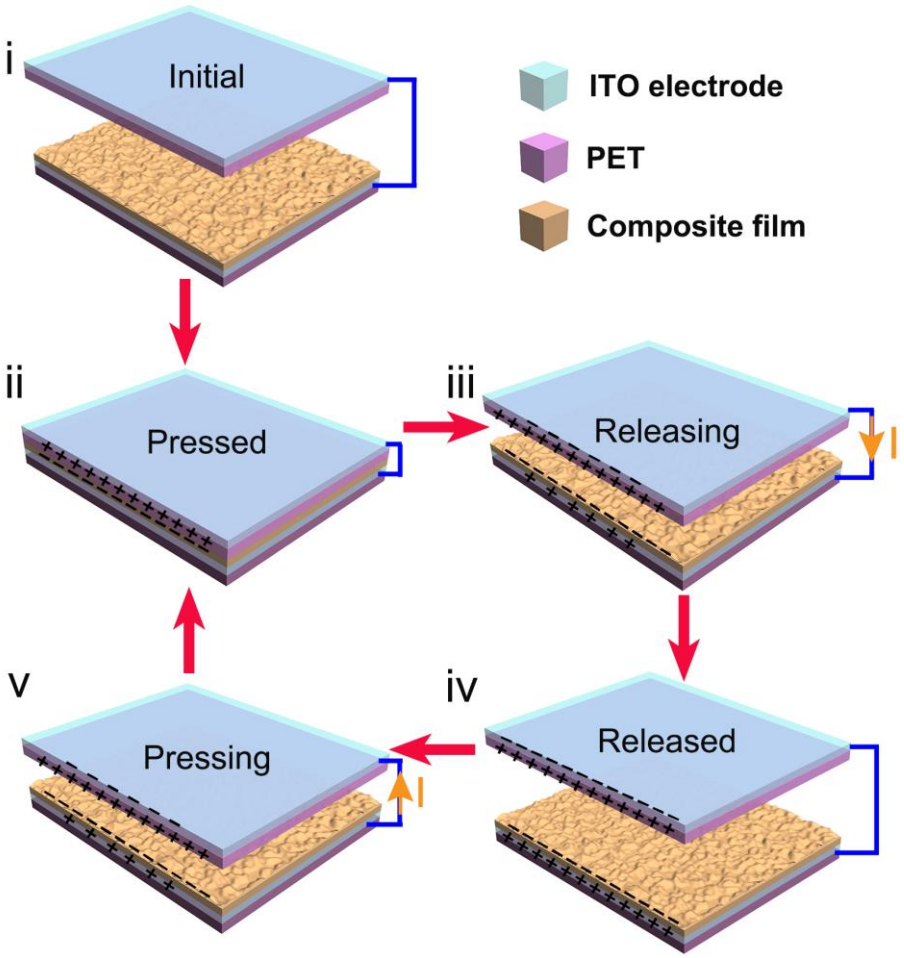

Figure 2. Fundamental working mechanism of polymer composite-based TENG. i) Original status without external force. ii) Contact status by pressing force, generating triboelectric charges. iii) Separation of friction layers, producing current flow through the external load. iv) The negative and positive friction layers completely returning back to the original status. v) The top film approaching the bottom film again, generating a reversed current flow.

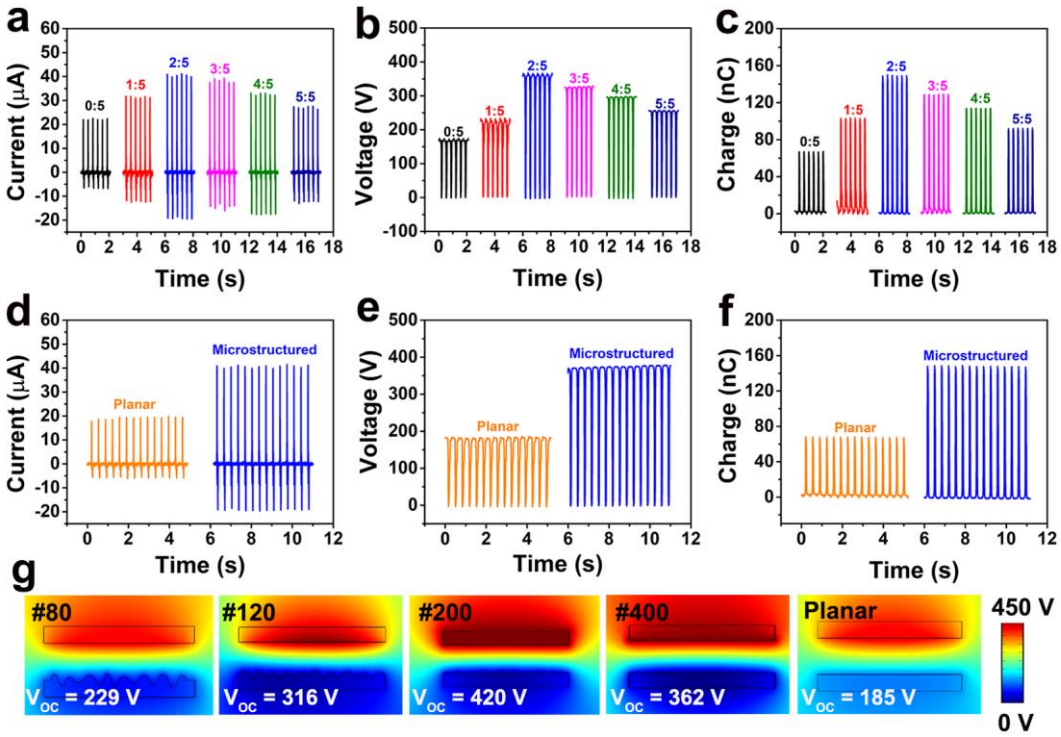

Figure 3. a-c) The output short-circuit current, output open-circuit voltage, and transferred charge of the TENGs based on G/PDMS composite films with various graphite concentrations. Comparsion of planar and microstructured G/PDMS composite film based TENGs in d) output short-circuit current, e) open-circuit voltage, and f) transferred charge, respectively. g) Simulation schematics of the TENGs based on #80, #120, #200 and #400 sandpaper developed microstructured and flat composite triboelectric layers.

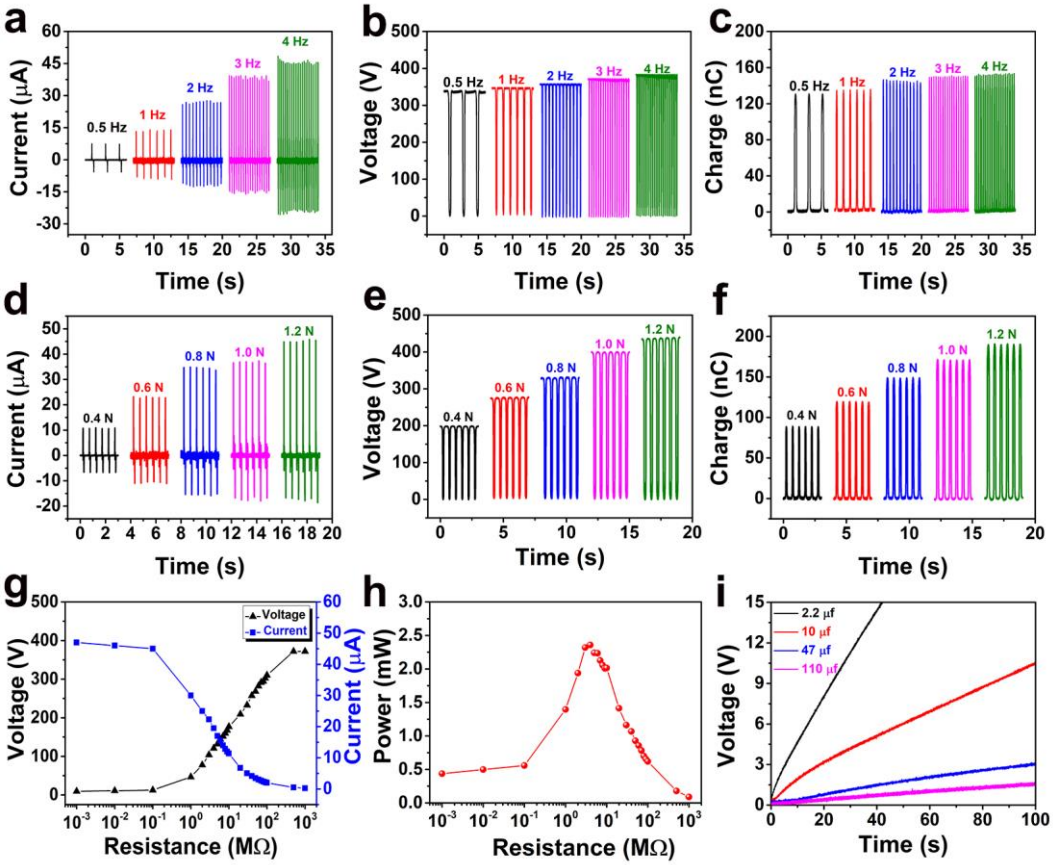

Figure 4. Electrical characterization of G/PDMS composite based TENG. Frequency dependence of a) short-circuit current, b) open-circuit voltage, c) transferred charges. External force dependence of d) short-circuit current, e) open-circuit voltage, f) transferred charges. g) Output voltage and current corresponding to different external load resistances under a contact-separation frequency of 3 Hz. h) Output power as a function of the loading resistance. i) The voltage curves of commercial capacitors (2.2, 10, 47, and 110 μF) charged by the TENG connected with a full bridge rectifier.

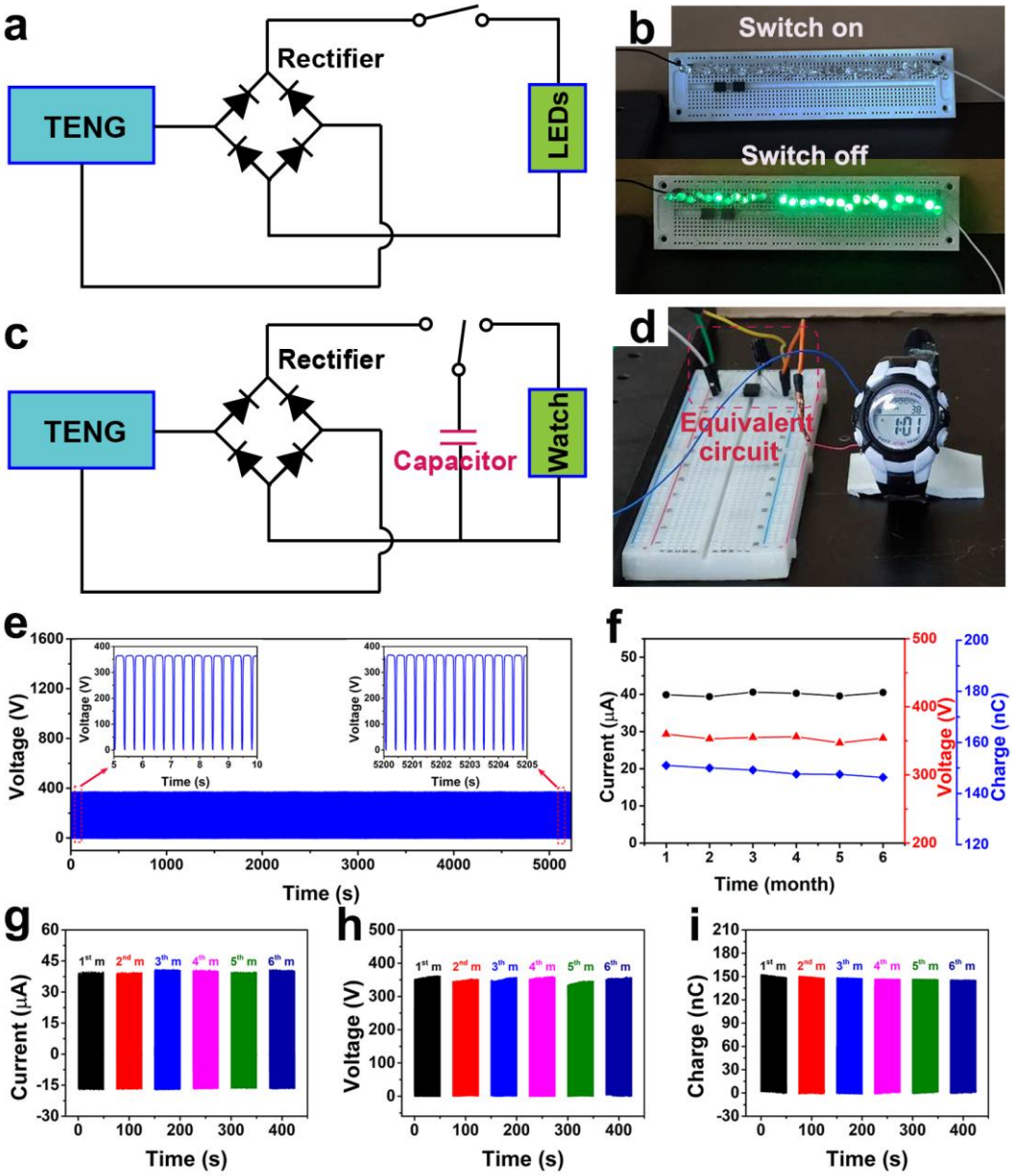

Figure 5. a) Schematic circuit diagram of full bridge rectifier with G/PDMS composite based TENG for driving commercial LEDs. b) Demonstration of 30 green LEDs connected in series powered by the TENG. c) Equivalent circuit diagram with G/PDMS composite based TENG for driving electronic watch. d) Demonstration of electronic watch driven by TENG. e) Voltage durability of TENG based on G/PDMS composite over 15, 000 cycles. Inset showing the enlarged view of voltage durability at the beginning and end of the test. f) The altitudes of current, voltage, and transferred charge over 6 months. g-i) Ambient stability of TENG in current, voltage, and transferred charge over 6 months.

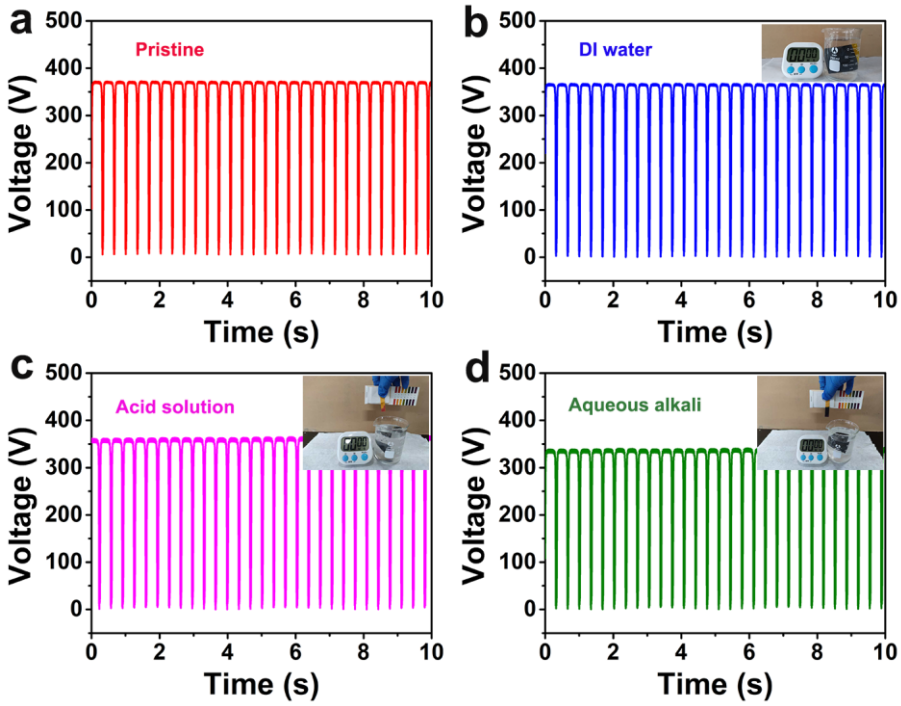

Figure 6. Output voltage characterizations of the a) pristine TENG, b-d) TENG with the composite layer soaked in DI-water, acid solution (PH~3) and acqueous alkali (PH~11) for 15 min, respectively. Insets in b-d showing the photographs of composite layer soaked in DI-water, acid solution and aqueous alkali, respectively.

Highlights

1. Scalable fabrication of the hierarchically microstructured G/PDMS composite films for high performance triboelectric nanogenerator.
2. An optimized polymer composite film achieving a maximum power of 2.4 mW under an external load of 3 MΩ.
3. Self-powered wearable sensors and self-charging systems.

Graphical Abstract

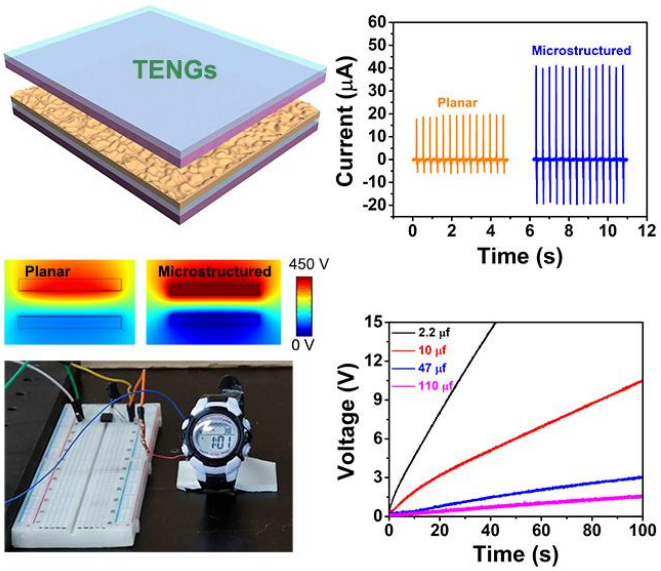

Scalable fabrication of hierarchically structured graphite/polydimethylsiloxane (G/PDMS) composite films for high-performance triboelectric nanogenerators (TENGs) has been demonstrated. The TENGs not only show a high output in I_{SC}, V_{OC}, and Q_T, but also exhibit excellent stability to the ambient conditions. The developed TENGs have demonstrated the applications in lightening commercial LEDs and charging the energy storage unit to drive wearable electronics.